Desalination and Water Treatment
www.deswater.com
1944-3994/1944-3986 © 2012 Desalination Publications. All rights reserved
doi: 10/5004/dwt.2012.2831

Taylor & Francis
Taylor & Francis Group

42 (2012) 333–346
April

Transport analysis of an air gap membrane distillation (AGMD) process

Mohammad Nurul Alam Hawlader[a,*], Rubina Bahar[b], Kim Choon Ng[b], Loh Jian Wei Stanley[b]

[a]*Department of Mechanical Engineering, International Islamic University Malaysia, Jalan Gombak, 53100 Kuala Lumpur, Malaysia Tel. +603 6196 6518; Fax: +603 6196 4455; emails: mehawlader@iium.edu.my, mnahawlader@gmail.com*
[b]*Department of Mechanical Engineering, National University of Singapore, 9 Engineering Drive 1, Singapore 117576*

Received 2 June 2011; Accepted 20 February 2012

ABSTRACT

Membrane distillation (MD) desalination is an emerging technology for fresh water production. This process incorporates phase change and transport of vapour through a hydrophobic membrane caused by vapour pressure across the membrane. The results from experimental studies and the one-dimensional transport analyses of the heat and mass transfer processes on an air gap MD (AGMD) unit are presented in this paper. The effects of different operating variables including feed and coolant temperatures, air gap, membrane support mesh size, feed concentration and feed and coolant flow rates were investigated. Mass transport through membrane, membrane support, air gap and condensation on the coolant plate has been analysed and expression for global mass transfer coefficient has been derived. The maximum distillate flux achieved was 5.11 kg m^{-2} h^{-1} at a feed temperature of 60°C, coolant temperature of 10°C and an air gap of 2.5 mm. Feed temperature and air gap width were found to have significant influence on the performance of the membranes.

Keywords: Membrane distillation (MD); Global mass transfer coefficient; Air gap membrane distillation (AGMD); Hydrophobic membrane; Mass transport through membrane; Polyvinylidene fluoride (PVDF) membrane

1. Introduction

Commercially available desalination processes mainly consist of thermal and membrane methods. Large-scale thermal distillation desalination requires large amounts of energy and special infrastructure that makes it fairly expensive compared to the use of natural fresh water. As a result, recently, membrane processes are taken into consideration and these processes rapidly grew as a major competitor to thermal desalination in the later years because of lower energy requirements, easier maintenance, smaller area, quicker start up and cost effectiveness, and thus leading to a reduction in overall desalination costs over the past decade. Most new facilities operate with reverse osmosis (RO) technology which utilizes semi-permeable membranes and high pressure to separate salts from water. However, RO process is not well-suited for hot or warm water as the membrane performance deteriorates with temperature above 40°C. With the burning issues of global warming, there has been a need to utilize the low grade waste heat before they can be released to the environment and a somewhat recent technique developed in the 1960s called Membrane Distillation (MD) shows good potential in utilizing low grade heat and producing fresh water from saline water.

*Corresponding author.

2011 Qingdao International Desalination Conference Symposium on Desalination and Water Treatment Global Platform for Water Solutions, June 20–23, 2011 Qingdao, China

The process uses the difference in partial pressure to produce vapour from a feed solution that gets condensed either by a direct cold distillate stream or a cold surface, and produces freshwater. To maintain the interfacial barrier between the two dissimilar temperature fluids, a hydrophobic membrane is required so that only the vapour can travel to the cold side.

The first MD patent was obtained in the early 1960s by Bodell [1]. By early 1980s the research on MD became very active with the advancement in polymer research that provided cheaper membranes. In the same decade, utilization of the low grade waste heat started to draw attention because of increased global warming. These issues caused the MD process to be revived after two decades since its discovery in the 1960s and different arrangements of the process like air gap MD and different structures of membranes including hollow fibre or spiral wound membranes were developed.

The major advantage of MD is its requirement of low grade energy associated with evaporation at ambient pressure. It is neither a high temperature process like (MED)/(MSF) nor does it require high pressure, as needed for RO process. Therefore, it is a very efficient method to utilize low grade waste/renewable energy including engine cooling water in a marine vessel, solar energy or even waste heat from condensers in an air conditioning system. As the determining factor for vapour generation is the partial pressure difference, the process is less sensitive to change in concentration. With development of hydrophobic membranes at a cheaper cost, MD process has been able to draw significant attention in contemporary water research. A cost analysis by Al-Obaidani et al. [2] showed that the total water production cost by MD is about 1.23 US$ m^{-3} (without using waste heat) while with waste heat and utilizing the energy from condensing steam, it can become as low as 0.26 US$ m^{-3} according to Meindersma et al. [3] .

Among different methods of MD air gap MD provides the advantage of increased heat transfer resistance between the hot and cold fluid. It also facilitates easier collection of distillate hence the chance of contamination of distillate by the feed water is less likely to occur. The process involves simultaneous heat and mass transfer through the membrane, the meshed membrane support and air gap. Alklaibi and Lior [4] presented the transport process in an AGMD process as a two-dimensional problem instead of one-dimensional transport assumed by Kimura and Nakao [5] and Schofield et al. [6]. However, in these studies, the membrane temperature has been estimated rather than direct measurement.

The work presented here describes experimental study on an AGMD unit along with a 1-dimensional model developed to validate the experimental results. Effects of different operating parameters including feed and coolant temperature, air gap width, membrane support mesh size, feed concentration and feed and coolant flow rates were investigated. Rather than estimating the temperatures at different locations of the module [7,8] the values were directly measured that accounted for all the heat losses from the system and also the temperature polarization. A one-dimensional vapour and heat transport mechanism through membrane, membrane support and air gap was investigated and experimentally found temperatures were used to express the partial pressure difference. The results obtained from the model were compared with experimental data. Improvement of the performance of MD system has been attempted in various methods including agitation of air gap [9], stirring of feed [10] or inclusions of spacers [11], however, the effect of support mesh size did not draw significant attention. Its influence on heat transfer has been discussed by Martinez-Diez and Florido-Diaz [12] considering the PTFE layer is the only part of the membrane participating in the water transport in vapour phase while substantial work has been presented by Courel et al. [13]. However, variation of effective diffusion coefficient with changing support mesh size was not reported. In the present study, an attempt was made to observe the effect of support mesh size and using the Global Mass Transfer Coefficient (GMC), the positive influence of bigger support mesh size on distillate production was demonstrated.

2. Working principle of air gap MD

In any MD process, the difference between the partial pressure on both side of membrane causes the hot saline feed water to evaporate. The vapour mass flux through membrane originates in the feed-membrane interface and then it passes through the pores in the hydrophobic membrane and support. After that, for an AGMD process the vapour travels across the air gap between membrane and coolant plate and, finally, condenses on the plate to produce distillate. Simultaneous heat and mass transfer occurs when the feed evaporates and travels through the membrane and air gap. Fig. 1 shows the process in details. The air gap situated between the membrane and the cold surface reduces energy loss caused by heat conduction through the membrane.

3. Experiments

A small experimental AGMD set up was built with Polyvinylidene Fluoride (PVDF) 0.45 μm pore size flat sheet membrane from Millipore Singapore. Further properties are tabulated in Table 1.

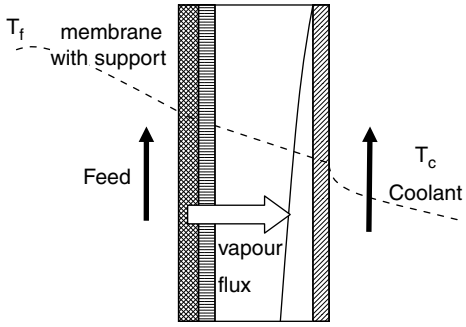

Fig. 1. Air Gap MD process.

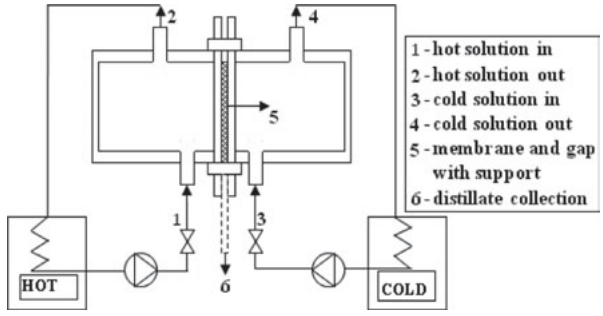

Fig. 2. Schematic diagram of the setup.

Table 1
Properties of durapore membrane

Water flow rate(ml min^{-1} cm^{-2})	35
Bubble point (bar)	≥0.56
Thickness (μm)	125
Effective membrane area (cm^2)	88.2
Membrane porosity	0.75

This disc shaped membrane was held between two Plexiglas tube chambers; one containing the hot feed while the other one was closed by the coolant plate at one end which faced the membrane to provide necessary cooling. This assembly formed the membrane module. The membrane was supported by a stainless steel mesh. The mesh was attached with the membrane using water resistant silicone sealant along the peripheral border while the membrane was pasted on a grooved flange and then the flange was attached to the feed chamber with silicone sealant. Between the membrane and the coolant plate, the desired air gap was maintained by insertion of gaskets. The vapour generated from hot feed passed through the membrane, then travelled through the air gap and condensed on the coolant plate. The distillate was collected by attaching a tube at the bottom of the coolant plate, where a small notch was cut in the gasket to make proper passage for the distillate to come out. Fig. 2 shows the schematic diagram of the setup. The air gap and the distillation collection path were properly sealed to secure no vapour escaping the system. A stainless steel plate was used as the coolant plate to avoid corrosion.

The membrane area, the vapour flow cross sectional area and the coolant plate area were identical in dimension. Temperature measuring points were tapped at different location including the membrane surface, air gap and coolant plate. Type T thermocouples were used with an accuracy of ±0.5°C. Once the procedure started, distillate drops were collected in a graduated tube. The operating variables included feed and coolant temperature, air gap width, membrane support mesh size, feed concentration and feed and coolant flow rates.

The mass flux calculation was directly related to partial pressure difference which again was dependent on the value of measured temperature. Hence, the experimental errors are caused by the measurement uncertainties in temperature and pressure. The instruments used in the experiments had the following uncertainties during measurement:

Thermocouple: ± 0.5°C.

Pressure gauge: ± 1% of gauge reading.

The instrument error δT_1 = ± 0.5°C is the uncertainty associated with the thermocouples, while the random error δT_2 is given by:

$$\delta T_2 = \sum_1^n \frac{\left(T - \overline{T}\right)}{n-1}$$

where n is the number of data taken to determine T, $\overline{T}$ is the mean of the population. The combined error is expressed as:

$$\delta T = \left(\delta T_1^2 + \delta T_2^2\right)^{0.5}$$

For the experimental measurement of the mass flux,

$$\dot{M}_{exp} = \frac{\text{distillate collected (kg)}}{\text{membrane area (m}^2\text{)} \times \text{time (s)}}$$

The distillate was collected in a graduated tube and the resolution was 1 ml. Hence, The uncertainties for measuring the mass flux (experimentally) = ± 0.5 ml. This value was considered to be constant for all experimentally obtained value of the mass flux.

4. Analyses

The vapour generated at the feed-membrane interface travelled through the membrane pores, membrane support meshes and the stagnant air gap consecutively. After the air gap, the vapour condensed on the coolant plate and a simple analysis of condensation on a vertical plate is included. Because of a narrow air gap, diffusion and conduction were considered as dominant transport processes. As the air was not agitated inside the air gap, hence, no mixing of vapour was assumed and the transport was considered to be one directional, that is, from membrane toward the coolant plate only. The generated vapour was considered to get condensed completely on the coolant plate.

4.1. Mass transfer process in AGMD

Fig. 3 shows the simultaneous heat and mass transfer through membrane, air gap and condensation on the coolant plate.

4.1.1. Mass transfer through membrane

Diffusion through a porous media like the membrane can be classified in main two classes based on pore size and mean free path, λ, which is described by Roque–Malherbe [14] as:

$$\lambda = \frac{3.2\,\mu}{P\sqrt{[RT/(2\,\pi M G_c)]}} \tag{1}$$

where G_c (an arbitrary constant) = 980 g mass-cm (g-force-s)$^{-2}$ and R = 84,780 g-force-cm (K-g-mol)$^{-1}$. The diffusion mechanism is determined based on the term

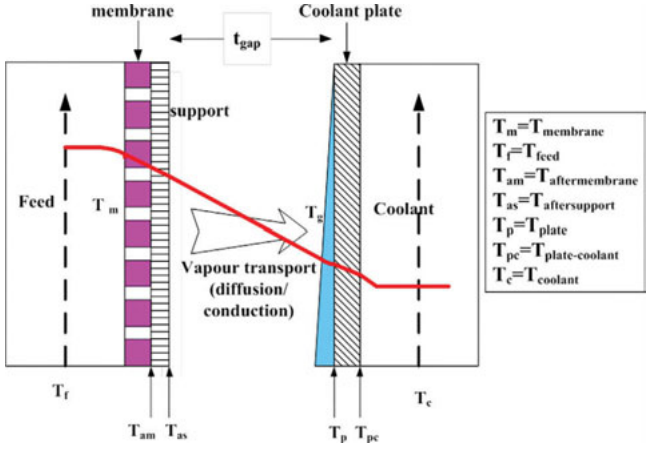

Fig. 3. Transport processes in AGMD.

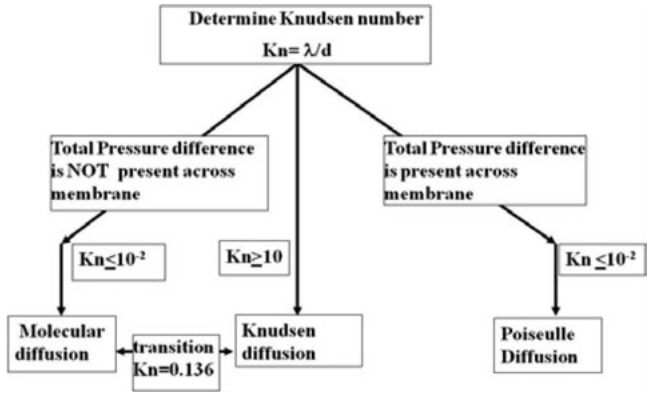

Fig. 4. Diffusion through membrane pores.

called Knudsen number which is expressed as $K_n = \lambda/d$. Fig. 4 shows a summary of different diffusion mechanisms that may occur through membrane pores based on K_n and pressure difference across the membrane.

The calculated mean free path was $\lambda = 6.13 \times 10^{-06}$ cm and K_n for this case was 0.136. Since, $10 \geq K_n \geq 10^{-2}$, the diffusion is a transition type between Knudsen and molecular diffusion. Once the diffusion process had been determined, the next step was to look for the diffusion coefficient for this transient diffusion.

Knudsen diffusion coefficient D_k is defined by Roque–Malherbe [14] as:

$$D_k = 9.7 \times 10^{-3}\,\frac{d}{2}\sqrt{\frac{T}{M}}\,\mathrm{m^2 s^{-1}} \tag{2}$$

For molecular diffusion of vapour thru' the air inside pores, the diffusion coefficient is given by Taylor and Krishna [15] as:

$$D_{AW} = 1.013 \times 10^{-2} \times T^{1.75}\,\frac{\sqrt{\left[\dfrac{M_w + M_a}{M_w M_a}\right]}}{P\left[\sqrt[3]{Z_w} + \sqrt[3]{Z_a}\right]} \tag{3}$$

where Z = molecular diffusion volumes of water and air (13.1 and 19.7), respectively. Scott and Dullien [16] gave a combined diffusion coefficient for transition between Knudsen and Molecular diffusion, which can be expressed as:

$$D_{combined} = \frac{D_{AW}}{a(Y_{w(m)} - Y_{w(am)})}\ln\left[\frac{1 - aY_{w(am)} + D_{AW}/D_k}{1 - aY_{(m)} + D_{AW}/D_k}\right] \tag{4}$$

where

$$a = \frac{1 + N_a}{N_w}$$

here, the vapour transport is dominant, hence the value N_a/N_w is considered to be negligible. According to Sherwood et al. [17] since the diffusion is taking place through pores, the porosity of membrane and tortuosity (as a measure of irregularity in shapes of the pores) is also considered and thus the diffusion coefficient becomes:

$$D_m = D_{combined} \times (\text{porosity}/\text{tortuosity}) \quad (5)$$

So the expression for water vapour molar flux as given by Scott and Dullien [16] as for Knudsen-molecular diffusion becomes:

$$\dot{M} = \frac{D_m}{RT_{avg}t_m} P\left[Y_{w(m)} - Y_{w(am)}\right] \quad (6)$$

here, $P = P_{atm}$.

The porosity and membrane thickness are known from the membrane manufacturer's data while the tortuosity value has been adopted from the work of Izquierdo-Gil et al. [18] with similar membrane. The mole fraction of vapour $Y_w = P_w/P_{atm}$, where P_w is the partial vapour pressure. Hence, the final expression for mass transfer through the membrane becomes in terms of partial pressure as:

$$\dot{M} = \frac{D_m}{RT_{avg}t_m}\left[P_{w(m)} - P_{w(am)}\right] \text{mole s}^{-1} \quad (7)$$

It is not easy to measure partial pressure of water vapour, but it can be expressed in terms of temperature by Antoine's relation for pure water where:

$$\log P_{w\text{-pure}} = \frac{B_1 - A_1}{(C_1 + T)} \quad (8)$$

here $B1 = 23.834$, $A1 = 3841$ and $C1 = 45$ [19].

When salt is present in the solution, the value of P_w is corrected using Raoult's law as:

$$P_w = (1 - CM_{NaCl})P_{w\text{-pure}} \quad (9)$$

here, CM = mole solute concentration.

However, as previously worked out by Alklaibi [20], Eq. (9) is not valid for higher concentration, and the value of P_w was used from the work of Fabuss ans Korosi [21] as:

$$k_w = \frac{P_{\text{pure-water}} - P_w}{m_w P_{\text{pure-water}}} \quad (10)$$

and

$$k_w = a + bg^{0.5}$$

here, k_w = relative molal vapour pressure depression, m_w = molality of solution, γ = Ionic strength of NaCl (for NaCl, γ = molar concentration); a and b are temperature dependant parameters expressed as $a = a_1 + a_2T + a_3T^2$ and $b = b_1 + b_2T + b_3T^2$.

And the mechanism Poiseuille–Knudsen diffusion for presence of pressure difference across membrane has been well worked by Schofield et al. [22]:

$$\dot{M} = \alpha \cdot p^b \, \Delta P \quad (11)$$

α = membrane permeation constant, $p = P/P_{ref}$ $b = 0$ (Knudsen diffusion); $b = 1$(Poiseuille flow) and P = pressure difference. The values of α and b were available for the same membrane from Ref. [22].

4.1.2. Mass transfer through membrane support and air gap

In AGMD process, a rigid support is needed to be attached with the membrane to hold the membrane against the feed flow and protect it from bulging. For the support, the mesh size was quite large compared to pore size of membrane and the K_n value falls dominantly in molecular transport region.

After passing through the support, the vapour travels through the air gap by molecular diffusion again as previously shown in Fig. 3. Both the mechanisms can be expressed by Stefan's law of molecular diffusion as Holman [23]:

$$\dot{M} = \frac{D_x P}{RT(P - P_w)} \frac{dP_w}{dy} \quad (12)$$

for the support, the value of $D_x = D_s$ and for the air gap, the value of $D_x = D_{AW}$ similar to membrane pores according to Sherwood et al. [17] D_s can be expressed as:

$$D_s = (\text{porosity}/\text{tortuosity})_{support} . D_{AW} \quad (13)$$

For the support, the vapour was passing not through any porous "medium", rather through a uniformly perforated plate with no irregularity; hence, the tortuosity is taken as one since there is no tortuous effect on the flow.

From Eq. (12), at steady state, $\dot{M}/dy = 0$

$$\frac{d}{dy}\left[\frac{D_x P}{RT(P-P_w)}\frac{dP_w}{dy}\right]=0$$

with the boundary condition for support as seen in Fig. 3
at $y = 0,\ P_w = P_{w(am)}$
at $y = t_s,\ P_w = P_{w(s)}$
and boundary condition for the air gap
at $y = 0,\ P_w = P_{w(s)}$
at $y = t_{gap},\ P_w = P_{w(p)}$

After integrating, for the membrane support:

$$\dot{M} = \frac{D_s C_v}{t_s}\ln\left(\frac{P_{w(s)}}{P_{w(am)}}\right) \tag{14}$$

and for the air gap:

$$\dot{M} = \frac{D_{AW} C_v}{t_{gap}}\ln\left(\frac{P_{w(p)}}{P_{w(as)}}\right) \tag{15}$$

where C_v is the molar concentration expressed as:

$$C_v = \frac{P}{RT_{avg}} \tag{16}$$

T_{avg} has been considered as the air gap temperature and $P = P_{atm}$ as the diffusion inside the air gap occurs at atmospheric pressure.

4.1.3. Mass transfer resistances and global mass transfer coefficient (GMC)

The mass transport and hence the production rate is also dependant on the mass transfer resistance offered by the membrane, the membrane support and the air gap. Only maintaining a specific partial pressure difference will not give the same production always as understood by the process of heat flow (temperature difference) or current flow (voltage difference). If the porosity of the membrane or the support mesh is changed, it will affect the total production. Therefore, an analysis of mass transfer resistance has been included and based on that, an expression of overall mass transfer coefficient from membrane to coolant plate has been derived.

a. Mass transfer resistance offered by membrane

From Eq. (7) the expression for molar flux through membrane can be expressed as:

$$\dot{M} = \frac{D_m}{RT_{avg}t_m}\left[P_{W(m)} - P_{W(am)}\right]$$

The mass transfer resistance can be written as:

$$r_m = \frac{RT_{avg}t_m}{D_m} \tag{17}$$

b. Mass transfer resistance offered by membrane support

The mass transfer resistance of the membrane support is derived by considering the partial pressure difference in Eq. (14) as driving force. Hence the expression for the resistance is obtained from Eq. (12) as:

$$r_{support} = \frac{RT_{avg}(P_{atm} - P_{w(avg)})t_s}{D_s P_{atm}} \tag{18}$$

c. Mass transfer resistance offered by air gap

Similar to $r_{support}$, for the air gap, the mass transfer resistance is expressed as:

$$r_{gap} = \frac{RT_{avg}(P_{atm} - P_{w(avg)})t_{gap}}{D_{AW}P_{atm}} \tag{19}$$

d. Global mass transfer coefficient

Combining Eqs. (17–19) gives the expression for GMC following heat transfer analogy as:

$$K_p = \frac{1}{r_m + r_{support} + r_{gap}} \tag{20}$$

Hence, the overall molar flux can be expressed in terms of overall mass transfer coefficient and partial pressure difference as:

$$\dot{M} = K_p \left[P_{w(m)} - P_{w(p)} \right] \text{mol s}^{-1} \quad (21)$$

With the help of Eq. (21), it would be possible to predict the effect of changing process parameters such as membrane and support porosity, air gap length etc inside the air gap. The mass flux in kg s^{-1} is be expressed as:

$$\dot{m}_c = \frac{\dot{M} \times 18}{1000} \text{ kg s}^{-1} \quad (22)$$

Finally, the product vapour flux can be calculated for passing through membrane, membrane support and air gap as:

$$J = \frac{\dot{M} \times 18}{1000 \times \text{membrane area}} \times 3600 \text{ kg m}^{-2}\text{h} \quad (23)$$

The properties of saline water have been taken from the work of Sharqawy et al. [24] for the necessary calculations.

The 1-D transport covers mainly diffusion for small air gap, for the case of convection inside a wider air gap, the mass transfer coefficient for air gap can be obtained from Reynolds analogy as given by Holman [23] for simultaneous heat and mass transfer as:

$$\frac{h}{h_m} = \rho C_p \left(\frac{Sc}{\text{Pr}} \right)^{2/3} = \rho C_p \left(\frac{\alpha}{D_{ab}} \right)^{2/3} \quad (24)$$

where h_m is the mass transfer coefficient. However, it is unusual to apply a wider air gap for any AGMD process as it actually offsets the advantage of the gap to reduce heat loss by increasing mass transfer resistance.

4.2. Heat transfer process in AGMD

The heat transfer process occurs in consecutive stages which include firstly the energy carried from the feed to the membrane surface followed by the heat transfer from membrane surface through membrane pores to the other side and then passing through membrane support and air gap before getting condensed on the coolant plate and finally carried away by the coolant flow. Since MD process involves simultaneous heat and mass transfer, the heat required for evaporation at the membrane surface has to be supplied from the bulk solution which creates a temperature gradient among the bulk fluid and the layer adjacent to membrane. This phenomena of temperature polarization expressed as:

$$\tau = \frac{T_m - T_p}{T_h - T_c} \quad (25\text{-a})$$

With lower temperature at the membrane–liquid interface, the partial pressure difference across the membrane reduces which causes decreased evaporation rate.

4.2.1. Heat transfer inside the feed chamber

The heat transfer equation inside feed chamber can be written as:

$$Q = h_{feed} A (T_{bulk} - T_m) + m \cdot c_{pL} (T_{bulk} - T_m) \quad (25\text{-b})$$

where h_{feed} = convective heat transfer coefficient and c_{pL}=specific heat in liquid phase. The value of h_{feed} for this specific design of feed chamber can be found from the correlation (Holman [23]) which gives:

$$\text{Nu} = 1.86(\text{Re Pr})^{1/3} \left(\frac{d_h}{L} \right)^{1/3} \left(\frac{\mu}{\mu_m} \right)^{0.14} \quad (26)$$

here μ and μ_m are the viscosities evaluated at bulk fluid temperature and membrane interface temperature, respectively.

4.2.2. Heat transfer through membrane

The heat transfer through membrane actually is a combined heat and mass transfer process and, therefore, involves the heat carried by the vapour mass along with the latent heat of evaporation. The mass to be evaporated comes to the feed membrane interface, evaporates there and travels through membrane, as shown in the following:

Total heat transferred at interface = sensible heat carried by the vapour + latent heat of evaporation, which gives:

$$Q = \left(\frac{k_{eff} A}{t_m} + \dot{m} c_{pg} \right) (T_m - T_{am}) + \dot{m} h_{fg} \quad (27)$$

here, k_{eff} = Effective membrane thermal conductivity that includes thermal conductivity of membrane material and vapour inside pores.

4.2.3. Heat transfer through membrane support

The vapour generated at the feed-membrane interface travels through the membrane and then passes through the membrane support. The heat transfer through the support takes the form as:

$$Q = \left(\frac{k_{\text{effsupport}} A}{t_s} + \dot{m} c_{pg} \right) \left(T_{am} - T_{as} \right) \quad (28)$$

here, $k_{\text{effsupport}}$ = effective conductivity of the support as it is a porous screen with air containing inside the pores, with the material conductivity taken as that of stainless steel.

4.2.4. Heat transfer through air gap

For the experimental range of temperature difference across the air gap and the width of air gap, the Rayleigh number value was below 1000 which indicated the heat transfer was dominate by conduction. For the transport through air gap, the heat transfer is expressed as:

$$Q = \left(\frac{k_a A}{t_{gap}} + \dot{m} c_{pg} \right) \left(T_{\text{aftersupport}} - T_g \right) \quad (29)$$

4.2.5. Heat transfer during condensation

The heat transfer coefficient for condensation has been determined using equations from Holman [23] where the coolant plate temperature is maintained at T_p and the vapour temperature at the edge of the film is T_g (for this case, the average air gap temperature has been considered from experimental data). The film thickness is represented by δ. The average value of heat transfer coefficient is obtained from integrating h(x) over the length of the plate L_p:

$$\bar{h}_c = \frac{1}{L_p} \int_0^{L_p} h_c(x) dx = \frac{4}{3} h_{c_{x=L_p}} \text{ Overall heat transfer}$$

$$Q = \bar{h}_c A (\bar{T}_g - \bar{T}_p) \quad (30)$$

the values of $\bar{T}_g$ and $\bar{T}_p$ were measured experimentally at the middle depth of the plate and air gap.

5. Results and discussion

Different operating parameters including feed temperature, coolant temperature, fluid flow rates, feed concentration, mesh size of membrane support and air gap thickness were varied and their effects on production were observed.

5.1. Effect of temperatures

The temperature of fluids dominates the distillate production rate by directly influencing the value of vapour partial pressure. By increasing only 15°C of the feed temperature, the production increased by 192%. While decreasing the coolant temperature enhanced the distillate flux, but the effect was not as significant as that of feed temperature. For a decrease of 15°C coolant temperature from 25°C to 10°C, distillate flux increased by 75%.

The production rates are observed for changing the feed and coolant temperatures in Fig. 5. With increased feed temperature, the vapour partial pressure at membrane surface increased. Since the vapour partial pressure depends on temperature exponentially, hence, a small rise in temperature enhanced the production significantly. MD process is dominated by the difference in partial pressure, which can be expressed in terms of temperature by exponential variation in Antoine's equation as described in Eq. (8). Hence, for same temperature difference, the production may vary depending on changing of feed or coolant temperature, as seen in Fig. 6. It is seen that for same temperature difference, the difference in partial pressure between two points may not be similar. And as a result, with same temperature difference,

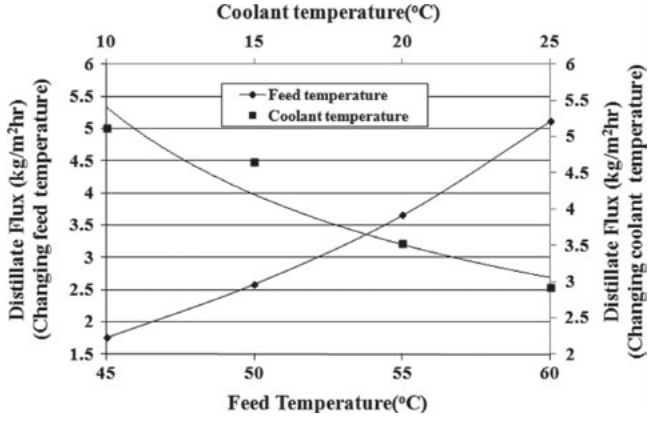

Fig. 5. Effect of changing feed temperature (T_c = 10°C and an air gap 2.5 mm).

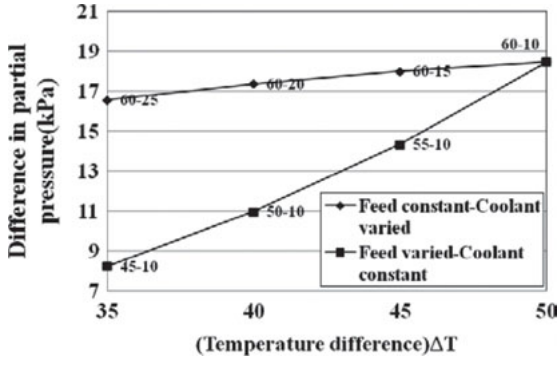

Fig. 6. Relation between partial pressure difference and temperature difference.

the production rate may be different depending on the side (feed/coolant) the temperature change takes place.

5.2. Effect of air gap

Air gap width is another dominating factor for production. Experiments conducted with changing air gap from 8.5 to 2.5 mm raised the flux by 158%. Fig. 7 shows the flux enhancement for changing air gap. This is attributed to the shortening of diffusion path length with decreased air gap width.

From the figure, it is seen that for air gap of 2.5 mm, the trend in change of flux with feed temperature was somewhat different compared to that of air gap of 5 and 8.5 mm. It may be predicted that for a thinner air gap, the mass transfer was dominated by diffusion while for wider gaps, convection started to take place and a linear trend of the distillate flux with increased temperature was observed.

5.3. Effect of feed concentration

There was a slight decrease in production with increasing feed concentration. Usually MD process is less sensitive to feed concentration as the driving force is partial pressure difference and it is determined based on Raoult's law of partial pressure. With increase in concentration of salt up to certain range (as long as it meets the criteria of dilute solution), mole fraction of water reduced insignificantly and, therefore, the effect of concentration was not very dominant on water production. Fig. 8 shows the effect of concentration on flux. However, Alklaibi [20] showed based on the data of Fabuss [21] that applying Raoult's law of partial pressure to determine interface temperature-concentration relation actually overestimates the flux.

5.4. Effect of flow rates

The feed flow rate did not show significant effect on distillate production. A little increase in production has been observed though with increasing the feed flow rate by four times. This slight increment in produced distillate can be linked to the experimental results from Matheswaran et al. [25]. It is seen from their work that, increasing the flow rate beyond 0.15 lpm caused the flux to reach a somewhat asymptotic value. The work of Garcia-Payo et al. [26] also supported the same trend. For the existing set up, the experimental range for feed flow rate, as seen in Fig. 9(a) , was within the limit of

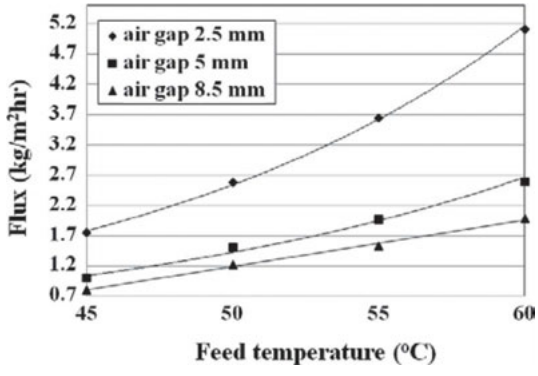

Fig. 7. Effect of changing air gap (coolant temperature = 10°C).

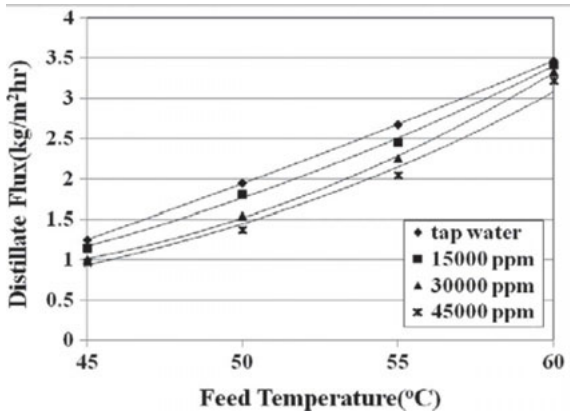

Fig. 8. Distillate flux with increasing feed concentration and temperature.

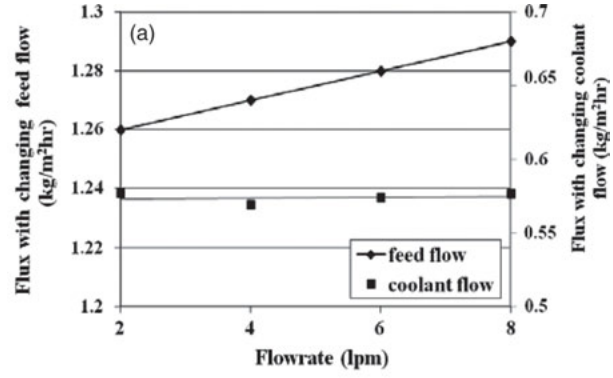

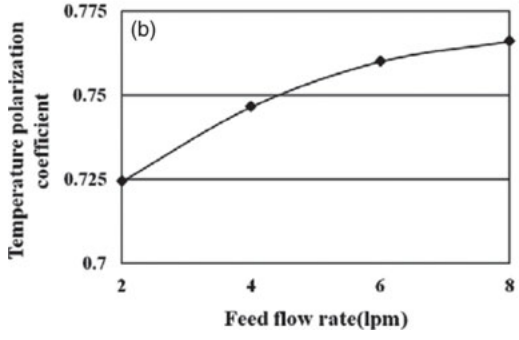

Fig. 9. (a) Variation in flux with increased feed and coolant flow (T_h = 55°C, T_c = 20°C, air gap = 7.5 mm). (b) Temperature polarization coefficient with increased feed flow.

2–8 lpm. It may be concluded that, for these flow rates (which already exceeded the previously stated values of flow rate), the asymptotic region was already reached and, therefore, only a small increment in the distillate flux has been observed which may be contributed by some degree of better mixing of fluids. The temperature polarization coefficient is plotted against flow rate in Fig. 9(b). And this figure indeed supports the possibility of better mixing as the polarization coefficient value increased slightly with increased feed flow rate. It was also investigated whether there was any effect of the coolant flow rate on the production as increasing coolant flowrate would increase heat transfer. The experimental results for increasing the coolant flowrate four times did not show any influence on the distillate production, as seen in Fig. 9(a). As the module chamber was small in height, and the coolat entry and exit temperature did not have large difference, the effect of coolant flow rate was less likely to have a significant effect on production rate. Since changing flowrates did not have any significant effect on production, further experiments (i.e., with different air gap width) were not conducted.

5.5. Effect of support mesh size

The support after the membrane offers some mass transfer resistance which is a part of the GMC and it may limit the ultimate distillate production by its mesh size. A stainless steel mesh with a porosity of 0.64 was tested as the membrane support and distillate flux obtained was compared with the membrane manufacturer's (Millipore Singapore) supplied membrane support which had a porosity of only 0.37. Although porosity does not have any direct control over the diffusion coefficient, D_{AW}, but when it comes to the expression of effective diffusion coefficient, only porosity is the dominating factor as found in Eq. (13) due to negligible non-uniformity(tortuous effect) for the support screen compared to that of membrane pores. Hence, the changing porosity of the support also controls the overall mass transfer resistance due to its change in the value of effective diffusion coefficient. From Fig. 10, it can be observed that the sieve support yields a higher flux than the Millipore support.

Table 2 shows the value of effective diffusion coefficient which caused the difference in production by manipulating the support resistance.

5.6. Mass transport resistances and global mass transfer coefficient

Analysis of the mass transfer resistance is important as it controls the overall mass transfer. It is seen in Fig. 11 that although membrane and support offer similar magnitude of resistances, the highest resistance of 7.63×10^5 J-s (m-mol)$^{-1}$ is offered by the 8.5 mm air gap because of longer diffusion path. Hence, the GMC thus reflects the advantage of having a narrower gap by showing the trend of about a three times higher value for air gap of 2.5 mm, compared to that of 8.5 mm.

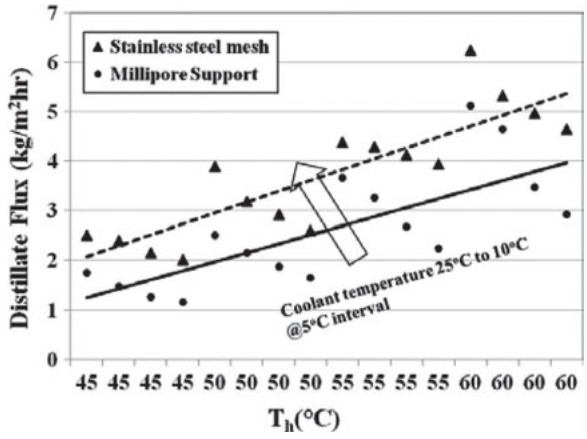

Fig. 10. Distillate flux enhancement with bigger mesh size stainless steel membrane support.

Table 2
Diffusion coefficients for two supports

T_h	T_c	Millipore support $D_{effective}$	Stainless steel mesh $D_{effective}$
45	10	8.72E-06	1.65E-05
45	15	8.76E-06	1.66E-05
45	20	8.79E-06	1.67E-05
45	25	8.79E-06	1.68E-05
50	10	9.01E-06	1.73E-05
50	15	8.97E-06	1.71E-05
50	20	8.95E-06	1.70E-05
50	25	8.92E-06	1.68E-05
55	10	9.14E-06	1.71E-05
55	15	9.18E-06	1.72E-05
55	20	9.23E-06	1.73E-05
55	25	9.26E-06	1.73E-05
60	10	9.41E-06	1.77E-05
60	15	9.30E-06	1.76E-05
60	20	9.30E-06	1.75E-05
60	25	9.25E-06	1.74E-05

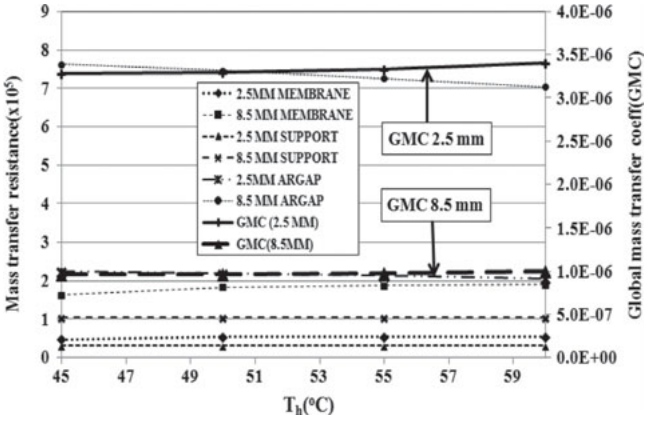

Fig. 11. The mass transfer resistances and GMC (for air gaps 2.5 and 8.5 mm).

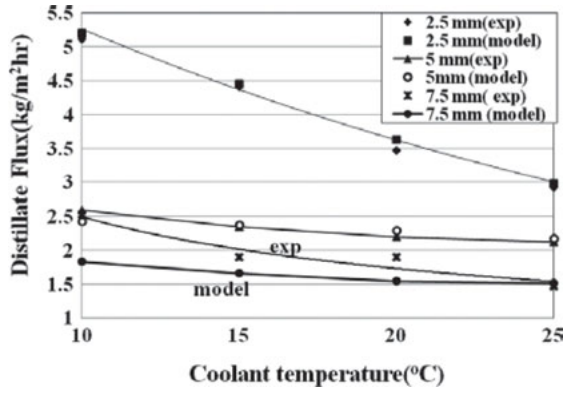

Fig. 13. Validation of production using 1-D model and deviation of production using 1-D model for a wider gap (air gap = 7.5 mm).

6. Validation of membrane and air gap transport using 1-D model

It is stated earlier that the temperature used in the validation of experimental results were obtained directly by tapping thermocouples at different locations of the test rig. As the production varies exponentially with temperature (Eq. (8)), the input value of temperature significantly affects the predicted value. The 1-D heat transfer equations were solved using MATLAB by Newton-Raphson method for the heat transfer from membrane until coolant side and theoretical values of temperature at different points were obtained.

Fig. 12 shows the temperature distribution obtained from simulation and experiments. The developed equations did not include any heat loss in the system, which is not the real case. Hence, the measured temperature magnitudes would give better prediction of production. Although there is a small variation between the simulated and experimental value, the transport equations are quite sensitive to the temperature magnitude and putting in the simulated values of temperature in the equation actually will over-predict the production. Using the experimental temperature values will lower the chance of over prediction.

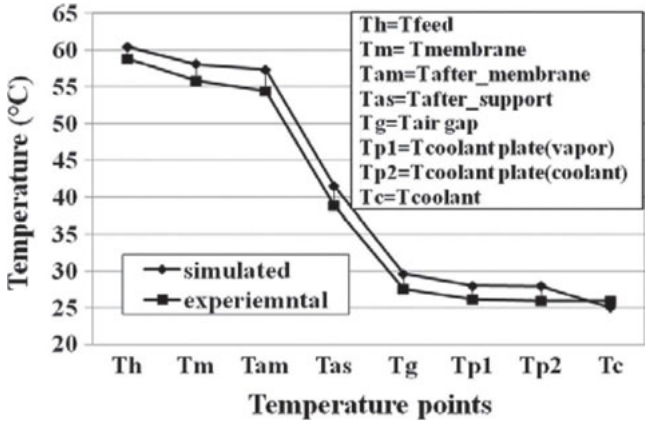

Fig. 12. Theoretical and experimental temperature distribution inside MD feed channel, air gap and coolant channel.

For validation of production, the overall mass transfer from membrane to coolant plate with 1-Dimensional diffusion was considered.

It is seen in Fig. 13 how the model was successfully implemented for air gap up to 6 mm but failed to predict the production for a higher air gap width of 7.5 mm. The 1-D equation was based on case of pure diffusion only, however, for a wider air gap, it is necessary to apply Reynold's analogy as stated earlier. But in practical application of AGMD,the air gap is kept to a lower value as its main purpose is to minimize the heat loss between the two fluids.

The effect of concentration becomes more severe at a higher feed concentration for MD process. To validate the experiemntal results, both Raoult's law of partial pressure and Fabuss' [21] experimental work were used in the 1-D model. It is found that for the expression of partial pressure, if Raoult's law is used for higher concentration, it fails to predict the values for concentration range beyond 30,000 ppm. So the 1-D model was corrected based on available data from Fabuss and the validation for the entire concentration range was in the satisfactory range. Fig. 14 shows the trend for both the cases.

7. Simulated results to predict the production based on membrane parameters

The influence of different membrane parameters on production were predicted based on the developed model. Since different types of hydrophobic membrane were not available from the supplier Millipore, there

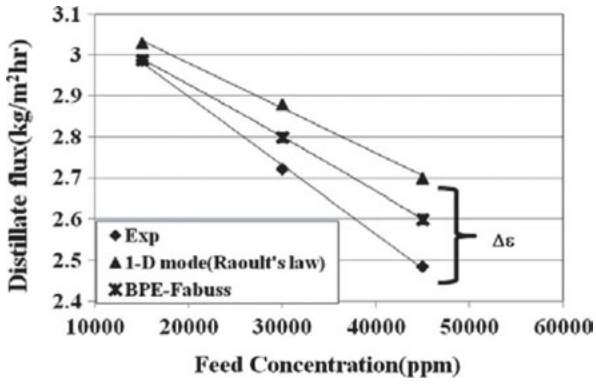

Fig. 14. Validation for increased feed concentration considering Raoult's law of partial pressure and BPE data from Fabuss.

was very limited scope to experimentally observe the effects of parameters like membrane thickness, porosity or thermal conductivity.

7.1. Effect of membrane thickness

Increasing the membrane thickness showed adverse effect on the production due to the contribution in increasing mass transfer resistance by longer diffusion path length as seen in Fig. 15. Similar experimental results have been reported by Al-Obaidani et al. [2]. Their study included changing the membrane thickness from 0.25 to 1.55 mm and a flux declination of 70% was observed. For the present study, similar declination is observed for increasing the membrane thickness from 0.15 to 1 mm.

7.2. Effect of membrane porosity

Membrane porosity was changed in the range from 0.1 to 0.9, without considering its effect on hydrophobic properties, and it shows that more porous membrane was producing more water as it influenced the diffusion coefficient directly. Besides, increasing membrane porosity also influenced the effective thermal conductivity of membrane, with increased porous zone; the conductivity of the vapour controlled the overall conductivity. Since, vapour thermal conductivity is less than the membrane thermal conductivity in magnitude, with increased porosity, the membrane was becoming more insulated and hence it added an extra advantage of reducing heat loss from membrane-liquid interface. Fig. 16 shows the distillate production trend with increased membrane porosity.

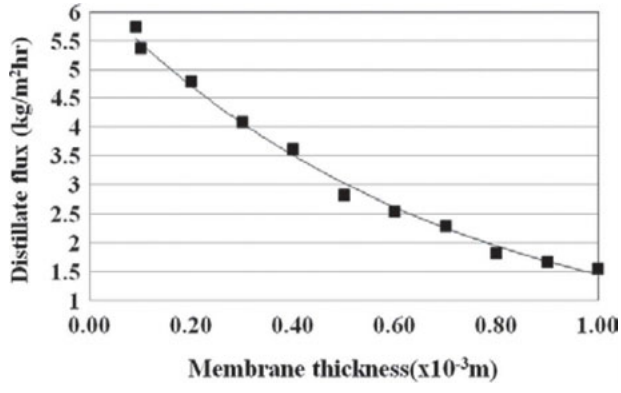

Fig. 15. Effect of membrane thickness on production. Feed 60°C, coolant 10°C, membrane porosity 0.75.

7.3. Effect of membrane thermal conductivity

As discussed in previous section, thermal conductivity plays a role in production by manipulating heat loss through membrane. Fig. 17 shows that with increased membrane thermal conductivity, for a certain membrane thickness, the production deteriorated as a result of more heat loss through membrane, thus losing the

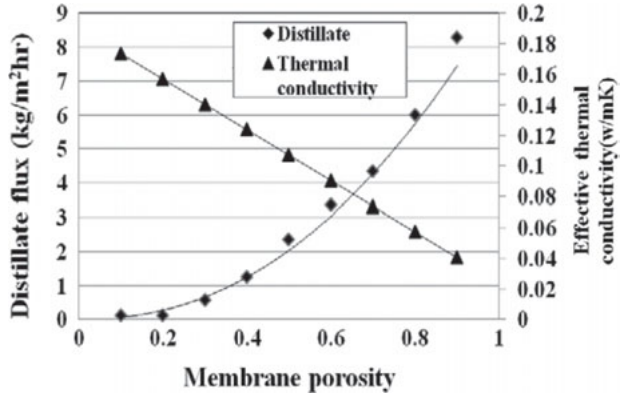

Fig. 16. Effect of membrane porosity on production. Feed 60°C, coolant 10°C, membrane thickness 125 × 10^{-6} m.

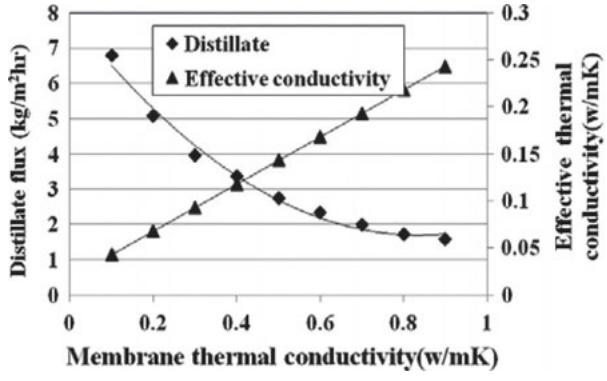

Fig. 17. Effect of membrane thermal conductivity on production. Feed 60°C, coolant 10°C, membrane porosity 0.75, thickness 125 × 10^{-6} m.

potential for evaporation. Similar trend is seen from the work of Alklaibi and Lior [4].

8. Conclusions

AGMD is a promising technology for desalination because of its low energy requirement and easy maintenance. Experimental and numerical investigations were carried out on a small scale AGMD unit. The process was not very sensitive to feed concentration and feed flow rate. The dominating factors for production were fluid temperatures and air gap width. The global mass transfer coefficient was derived using the mass transfer resistances offered by membrane, membrane support and air gap. The changing porosity of the membrane support controlled the production significantly due to its change in the value of effective diffusion coefficient. The numerical results showed good agreement with experimental values. For an air gap of 2.5 mm and feed temperature of 60°C and coolant temperature of 10°C, the highest flux obtained was 5.11 kg m^{-2} h^{-1}.

Symbols

A — Area [m^2]
d — Diameter of membrane pore [m]
D — Diffusion coefficient [m^2/s]
h — Heat transfer coefficient [W/m^2K]
h_c — Condensation heat transfer coefficient [W/m^2K]
h_{fg} — Latent heat of evaporation [J/kg]
J — Distillate flux [kg/m^2h]
k — Thermal conductivity [W/mK]
K_u — Knudsen number
K_p — Global mass transfer coefficient [mole-m/j-s]
$\dot{m}$ — Mass flux of water vapour [kg/s]
$\dot{M}$ — Molar flux of water vapour [moles/s]
M — Molar weight [kg/mole]
N — Molar flux [moles/s]
Nu — Nusselt Number
P — Pressure [Pa]
Pr — Prandtl Number
P_w — Partial vapour pressure [Pa]
Q — Heat transfer rate [W]
R — Universal gas constant (J/K-mole)
Re — Reynolds Number
Sc — Schmidt Number
T — Temperature [K]
t — Thickness/width [m]
Y_w — Mole fraction of vapour

Greek letters

α — Thermal diffusivity, (m^2/s)
β — Thennal expansion coefficient
δ — Condensate film thickness (m)
γ — Ionic strength (mole/l)
λ — Mean free path (cm)
μ — Dynamic viscosity (N-s/m^2)
ρ — Density (kg/m^3)

Subscripts

a — Air
AW — Diffusivity of vapour in air
am — After membrane
as — After support
avg — Average of two boundaries
g — Gas/water vapour
gap — Air gap
if — Interface
m — Membrane
P — Plate
s — Membrane support
sol — Solution
w — Water

References

[1] B.R. Bodell, Silicon rubber vapour diffusion in saline water distillation, United States Patent Serial No. 285,032, 1963.
[2] S. Al-Obaidani, E.C.F. Macedonio, G. Di Profio, H. Al-Hinai and E. Drioli, Potential of membrane distillation in seawater desalination: Thermal efficiency, sensitivity study and cost estimation, J. Membr. Sci., 323 (2008) 85–98.
[3] G.W. Meindersma, C.M. Guijt and A.B. de Haan, Desalination and water recycling by air gap membrane distillation, Desalination, 187 (2006) 291–301.
[4] A.M. Alklaibi and N. Lior, Transport analysis of air-gap membrane distillation, J. Membr. Sci., 255 (2005) 239–253.
[5] S. Kimura and S. Nakao, Transport phenomena in membrane distillation, J. Membr. Sci., 33 (1987) 285–298.
[6] R.W. Schofield, A.G. Fane and C.J.D. Fell, Heat and mass transfer in membrane distillation, J. Membr. Sci., 33 (1987) 299–313.
[7] A.M. Alklaibi and N. Lior, Heat and mass transfer resistance analysis of membrane, Distillation, J. Membr. Sci., 282 (2006) 362–369.
[8] L. Martinez, Comparison of membrane distillation performance using different feeds, Desalination, 168 (2004) 359–365.
[9] R. Chouikh, S. Bouguecha and M. Dhahbi, Modelling of a modified air gap distillation membrane for the desalination of seawater, Desalination, 181 (2005) 257–265.
[10] M.P. Godino, L. Pena, C. Rincon and J.I. Mengual, Water production from brines by MD, Desalination, 108 (1996) 91–97.
[11] M.N. Chernyshov, G.W. Meindersma and A.B. de Haan, Modelling temperature and salt concentration distribution in MD feed channel, Desalination, 157 (2003), 315–324.
[12] L. Martinez-Diez and F.J. Florido-Diaz, Desalination of brines by MD, Desalination, 137 (2001) 267–273.
[13] M. Courel, M. Dornier, G.M. Rios and M. Reynes, Modelling of water transport in osmotic distillation using asymmetric membrane, J. Membr. Sci., 173 (2000) 107–122.
[14] R.M.A. Roque-Malherbe, Adsorption and Diffusion in Nanoporous Materials, CRC Press, Taylor & Francis Group, Florida, 2007.
[15] R. Taylor and R. Krishna, Multi-component Mass Transfer, Wiley Series in Chemical Engineering, John Wiley, New York, 1993.
[16] D.S. Scott and F.A.L. Dullien, Diffusion of ideal gases in capillaries and porous solids, AIChE, 8(1) (1962) 113–117.

[17] T.K. Sherwood, R.L. Pigford and C.R. Wilke, Mass Transfer, McGraw-Hill, New York, NY, 1975.
[18] M.A. Izquierdo-Gil, M.C. Garcia-Payo and C. Farnandez-Pinenda, Air gap membrane distillation of sucrose aqueous solutions, J. Membr. Sci., 155 (1999) 291–307.
[19] J.M. Smith, Introduction to Chemical Engineering Thermodynamics, 3rd Edition. McGraw Hill, NY, 1981.
[20] A.M. Alklaibi, Desalination by membrane distillation, PhD Thesis, University of Pennsylvania, Philadelphia, USA, 2004.
[21] B.M. Fabuss and A. Korosi, Vapor pressures of binary aqueous solutions of NaCl, KCl, Na_2SO4 and $MgSO_4$ at concentrations and temperatures of interest in desalination processes, Desalination, 1 (1966) 139–148.
[22] R.W. Schofield, A.G. Fane and C.J.D. Fell, Gas and vapour transport through microporous membranes. I. Knudsen-Poiseuille transition, J. Membr. Sci., 53 (1990) 159–171.
[23] J.P. Holman, Heat Transfer, 5th edition, McGraw-Hill, New York, 2002.
[24] M.H. Sharqawy, V.J.H. Lienhard and S.M. Zubair, Thermophysical properties of seawater: A review of existing correlations and data, Desalin. Water Treat., 16 (2010) 354–380.
[25] M. Matheswaran, T.O. Kwon, J.W. Kim and I.S. Moon, Factors affecting flux and water separation performance in air gap membrane distillation, J. Ind. Eng. Chem., 13 (2007) 965–970.
[26] M.C. Garcia-Payo, C.A. Rivier, I.W. Marison and U. Von Stockar, Separation of binary mixtures by thermostatic sweeping gas membrane distillation: II. Experimental results with aqueous formic acid solutions, J. Membr. Sci., 198 (2002) 197–210.